

# CHARACTERIZATION OF ATOMIC-LAYER-DEPOSITED NbTiN AND NbTiN/AlN FILMS FOR SIS MULTILAYER STRUCTURES\*

Z. Sun<sup>†</sup>, M. U. Liepe, T. Oseroff, CLASSE, Cornell University, Ithaca, New York  
X. Deng, Chemical Engineering, University of Virginia, Charlottesville, Virginia

## Abstract

SIS (superconductor-insulator-superconductor) multilayer structures are proposed designs to repel early flux penetration and ease the impact of defects in SRF cavities. The demonstration of such device physics is strongly affected by the film qualities – material structure and composition. Here, we characterized 100 nm NbTiN / 2 nm AlN / bulk Nb SIS structures and investigated the effect of the presence of the AlN layer on the NbTiN film properties. We find that the hcp-structured AlN layer results in a Nb composition gradient as a function of film depth, whereas the Nb concentration remains constant in the NbTiN/Nb samples, which suggests that interface mismatch could induce significant change in NbTiN composition. The surface composition variation further leads to different oxide structures, which might impact the superconducting performance. Our observations indicate that the choice of the insulating layer in SIS structures is critical, and that interface mismatch together with internal strain could deteriorate the superconducting film.

## INTRODUCTION

SIS structures proposed by A. Gurevich [1] take advantage of an insulating (I) layer between a thin superconducting (S) film and the superconducting (S) Nb bulk. Through optimizing the topmost superconducting film thickness versus the London penetration depth [2,3], the SIS design could repel vortex penetration and support increased surface magnetic field. To experimentally validate the device physics, researchers have explored superconducting films such as NbN [3-5], NbTiN [5-7], and Nb<sub>3</sub>Sn that have larger penetration depths ( $\lambda$ ) and higher critical temperatures ( $T_c$ ) than Nb.

However, the film quality is critical to effectively test the RF performance of SIS structures. Variation could be from two resources: material issues (stoichiometry, phase, and surface oxide) or multilayer design issues (choice of superconducting and insulating films, and their thickness), both of which should be prioritized to test a rational SIS design. Otherwise, for example, the material issue may become a dominant factor, when the field for vortex penetration does not achieve the theoretical predications [5,8,9].

Atomic layer deposition (ALD) for fabricating SIS structures recently attracts attention owing to the atomic-scale

control of thickness and composition. Characterization of ALD-based SIS structures has not been extensively studied, while researchers have optimized sputter-based SIS structures [3,4,7-9]. Also, the role of the insulating layer as an intermediate layer during deposition is not clear yet. Interface characterization would facilitate future optimization of the deposition process.

In this work, ALD NbTiN/AlN films on the Nb substrate were characterized via elemental depth profiling and X-ray diffraction. Stoichiometry, phase structure, and surface oxides were determined. The influence of the AlN layer on the deposition was revealed by comparing results with NbTiN reference films directly grown on Nb surfaces.

## EXPERIMENTAL PROCEDURES

The SIS films were prepared using a plasma-enhanced ALD system by Mark Sowa (Veeco-CNT). Two film structures (100 nm NbTiN / 2 nm AlN / bulk Nb vs. 100 nm NbTiN / bulk Nb) were fabricated as shown in Fig. 1.

A Zeiss Gemini 500 scanning electron microscope (SEM) was used to examine the surface morphology and grain size. Depth profiling via X-ray photoelectron spectroscopy (XPS) was performed to provide the stoichiometry as a function of the film depth. X-ray diffraction (Rigaku XRD) was used to probe the phase information.

## RESULTS AND DISCUSSION

### Surface Morphology and Grain Size

Figure 1 shows a comparison of surface morphology for NbTiN/AlN/Nb and NbTiN/Nb structures. Both films are smooth, while the grain size (~4 nm) is small. In literature, grain sizes ranging from 20 nm to 170 nm were reported for the sputtered NbTiN films [7,10]. Our results suggest post annealing is preferred to promote grain growth, leading to a lower density of grain boundaries.

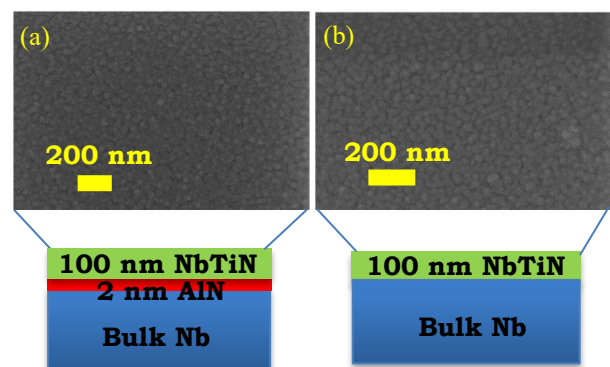


Figure 1: SEM surface morphology for (a) NbTiN/AlN/Nb structures and (b) NbTiN/Nb structures.

\* This work was supported by the U.S. National Science Foundation under Award PHY-1549132, the Center for Bright Beams. Also, this work made use of the Cornell Center for Materials Research Shared Facilities which are supported through the NSF MRSEC program (DMR-1719875), and was performed in part at the Cornell NanoScale Facility, an NNCI member supported by NSF Grant NNCI-2025233.

<sup>†</sup> zs253@cornell.edu

## Elemental Depth Profiling

XPS depth profiling of both NbTiN/AlN/Nb and NbTiN/Nb films was performed to study the stoichiometric and chemical variation between the two structures. After sputtering away 96 nm of the NbTiN/AlN surface, Al 2p signal started to appear under XPS, which suggests the actual interface between NbTiN and AlN films. Figure 2 plots the Nb, Ti, and N spectra at four representative depth locations from the outmost surface, 0 nm, to the film interface, 96 nm. Except the distinctive variation observed at the outmost surface owing to oxidization, we find that the Ti and N peak intensities are essentially constant all through the film for both samples. By contrast, the Nb peak intensity drops originating from the film interface toward the outer surface in the NbTiN/AlN/Nb samples, while such Nb composition gradient is not observed in the NbTiN/Nb samples. This behavior strongly suggests that the hexagonal-structured AlN layer, that is different from the cubic-structured Nb, plays an important role in determining the stoichiometry of the subsequently deposited NbTiN film.

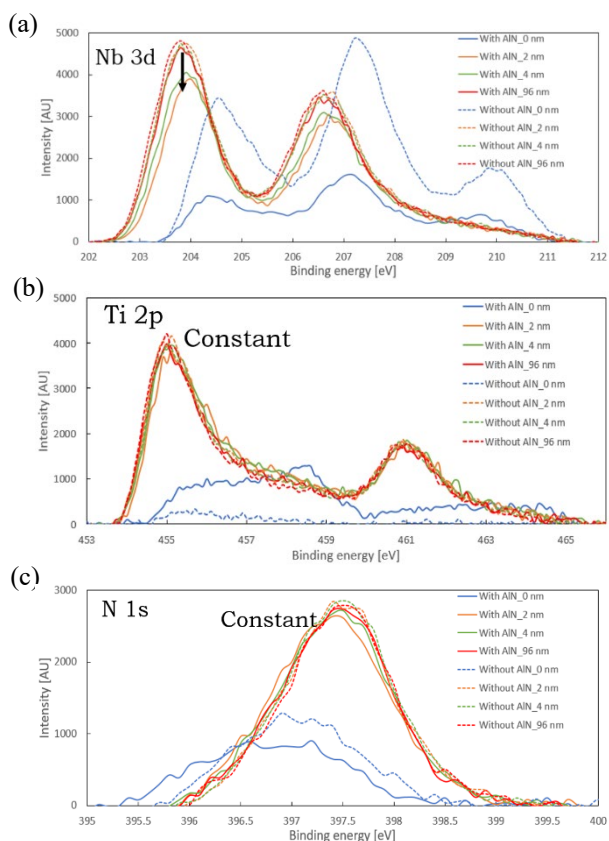


Figure 2: XPS depth profiling of (a) Nb 3d, (b) Ti 2p, and (c) N 1s from the outmost surface (0 nm) to the film interface (96 nm) for both NbTiN/AlN/Nb (with AlN) and NbTiN/Nb (without AlN) samples.

Further quantification of the composition as a function of depth (Fig. 3a) shows that the Nb composition decreases from 25% at the depth of 96 nm, to 20% at the surface for NbTiN/AlN/Nb samples, as the Ti and N compositions accordingly increase. By normalizing the absolute XPS peak

intensities to the interface values, Fig. 3b confirms a relative change of nearly 20 % for the loss of Nb content at the surface of NbTiN/AlN/Nb films.

The reference NbTiN/Nb samples show a constant stoichiometry of Nb<sub>0.53</sub>Ti<sub>0.59</sub>N through the film. Results infer that N deficiency exists in both samples, while the Ti fraction is larger than the optimum 0.3-0.4 values. Previous studies [11-13] proved that the critical temperature and surface resistance of NbTiN films depend on the Ti fraction but scattered results were reported. Di Leo's results [11] showed a high critical temperature of 17 K at below 0.5 Ti fractions, while Tsavdaris [12] observed the best T<sub>c</sub> of 13 K for their chemical vapor deposited films at the 0.46 Ti fraction. In addition, Yu's work [13] showed ~0.34 Ti fraction yielded their highest T<sub>c</sub> of 16 K in the sputtered films. Although scattered, these results suggest NbN/TiN ratios above 1 are expected to increase the critical temperature of NbTiN films, which was not achieved in this work and requires further optimization of the deposition process.

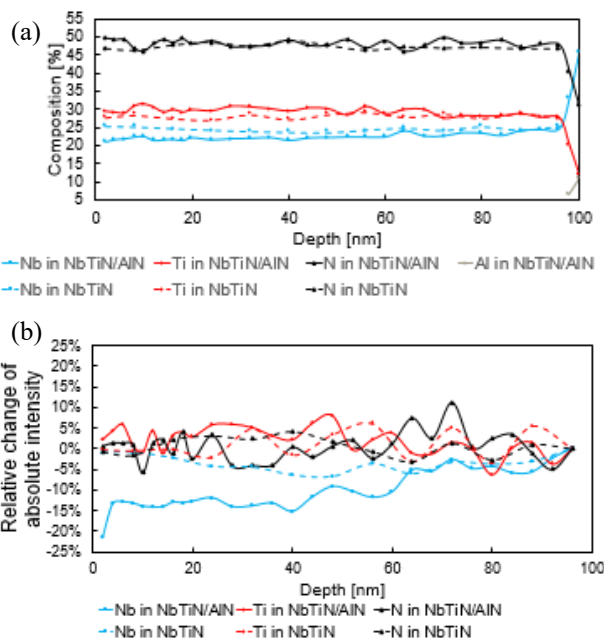


Figure 3: (a) Composition depth profiles and (b) relative change of XPS peak intensities of Nb, Ti, N, and Al for NbTiN/AlN and NbTiN-only films on Nb substrates. The absolute peak intensities were normalized to the interface values at the depth of 96 nm.

## Phase Structure

To analyze the reasons for composition variation in both films, X-ray diffraction was conducted to identify the phase structures. Fig. 4 shows the hcp-AlN diffraction was only observed in the NbTiN/AlN film. Due to the presence of this hexagonal AlN structure, the top NbTiN film produced both cubic and hexagonal diffractions. On the contrary, the NbTiN-only film, thanks to the cubic Nb structure, is able to retain the cubic structure.

Indeed, the choice of crystal structure for the thin insulating layer is critical. Studies by Makise [10] showed that

Content from this work may be used under the terms of the CC BY 4.0 licence (© 2022). Any distribution of this work must maintain attribution to the author(s), title of the work, publisher, and DOI

NbTiN deposition on a cubic MgO substrate yielded completely different diffraction patterns compared to depositions on a hexagonal Al<sub>2</sub>O<sub>3</sub> substrate or on a fused quartz substrate. Epitaxy of cubic (200) NbTiN films was achieved on the cubic (100) MgO surface [10]. Similar results were also reported by Jefferson Lab [7]. Such epitaxial growth is preferred since the cubic NbTiN has a high T<sub>c</sub> and it avoids the disorders such as stoichiometry variation and phase fluctuation that were induced by the interface mismatch in a chemical vapor process.

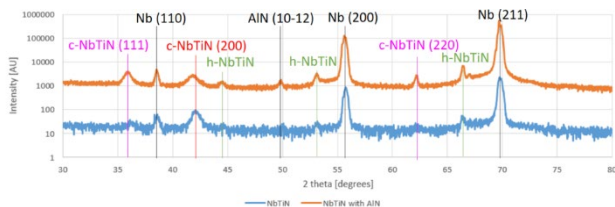


Figure 4: XRD patterns for NbTiN/AlN and NbTiN-only films on Nb substrates.

### Surface Oxides

As shown in Fig. 2, the outermost surfaces exhibit distinctive oxide structures, and the surface oxides differ between NbTiN/AlN and NbTiN-only films. These surface oxides as a possible normal conducting region are of interest. Through XPS spectrum fitting [14-16], the oxide, nitride, and oxynitride structures were deconvoluted as shown in Fig. 5. Due to the Nb deficiency, Ti-related oxides predominate on the NbTiN/AlN surface. By contrast, the Nb-related oxides primarily exist on the NbTiN-only surface, together with nearly no Ti-related oxides. The effect of such oxide variation deserves further investigation.

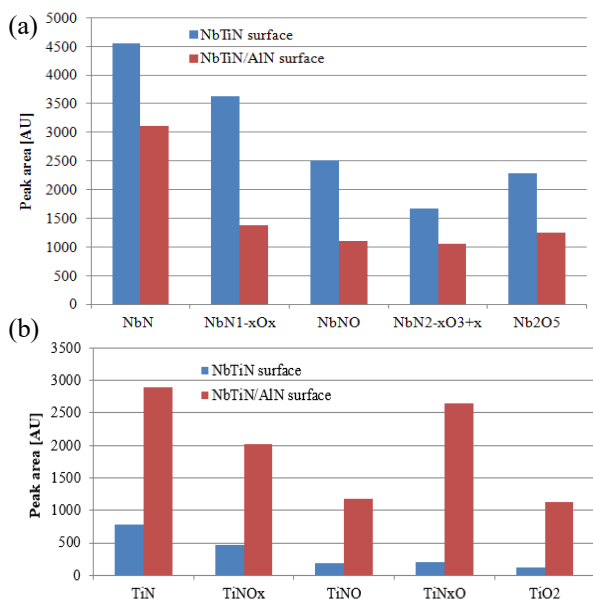


Figure 5: (a) Nb-related and (b) Ti-related surface oxides, nitrides, and oxynitrides for NbTiN/AlN and NbTiN-only films on Nb substrates.

## CONCLUSIONS

ALD NbTiN/AlN/Nb SIS structures were characterized and compared with a reference NbTiN/AlN structure. We find that the hexagonal-structured AlN insulating layer is critical to determining the subsequently deposited NbTiN phase. Mixed cubic and hexagonal structures were observed in the NbTiN films in presence of an hcp-AlN layer, while the preferred cubic structure could be retained on the cubic Nb surface, suggesting epitaxial growth on a cubic insulating layer is preferred. Moreover, the Nb concentration gradient was observed in the NbTiN/AlN samples along with a decreased value toward the surface. The stoichiometry in both films is not at the optimum and requires future optimization. Also, due to the stoichiometry variation, surface oxides on both films differed. In summary, choice and optimization of the thin insulating layer is required in SIS structure fabrication.

## REFERENCES

- [1] A. Gurevich, "Enhancement of rf breakdown field of superconductors by multilayer coating", *Appl. Phys. Lett.*, vol. 88, 012511, 2006. doi:10.1063/1.2162264
- [2] T. Kubo *et al.*, "Radio-frequency electromagnetic field and vortex penetration in multi-layered superconductors", *Appl. Phys. Lett.*, vol. 104, 032603, 2014. doi:10.1063/1.4862892
- [3] H. Ito *et al.*, "Lower critical field measurement of NbN multilayer thin film superconductor at KEK", in *Proc. 19th Int. Conf. on RF Superconductivity (SRF'19)*, Dresden, Germany, Jun. 2019, pp. 632-636. doi:10.18429/JACoW-SRF2019-TUP078
- [4] S. Leith *et al.*, "Superconducting NbN thin films for use in superconducting radio frequency cavities", *Supercond. Sci. Technol.*, vol. 34, 025006, 2021. doi:10.1088/1361-6668/abc73b
- [5] T. Oseroff *et al.*, "RF characterization of novel superconducting materials and multilayers", in *Proc. 19th Int. Conf. on RF Superconductivity (SRF'19)*, Dresden, Germany, Jun. 2019, pp. 950-955. doi:10.18429/JACoW-SRF2019-TUP044
- [6] Z. Sun *et al.*, "Study of alternative materials for next generation SRF cavities at Cornell University", presented at *9th Int. workshop on thin films and new ideas for pushing the limits of RF Superconductivity*, Mar. 2021. <https://indico.jlab.org/event/405/contributions/7865/>
- [7] M. C. Burton *et al.*, "Superconducting NbTiN thin films for superconducting radio frequency cavity applications", *J. Vac. Sci. Technol. A*, vol. 34, 021518, 2016. doi:10.1116/1.4941735
- [8] M. R. Beebe *et al.*, "Stoichiometry and thickness dependence of superconducting properties of niobium nitride thin films", *J. Vac. Sci. Technol. A*, vol. 34, 021510, 2016. doi:10.1116/1.4940132
- [9] S. Keckert *et al.*, "RF characterization of an S-I-S' multilayer sample", in *Proc. 19th Int. Conf. on RF Superconductivity (SRF'19)*, Dresden, Germany, Jun. 2019, pp. 800-806. doi:10.18429/JACoW-SRF2019-THFUA1

- [10] K. Makise *et al.*, “Characterization of NbTiN thin films deposited on various substrates”, *IEEE Trans. Appl. Supercond.*, vol. 21, pp. 139-142, 2011.  
doi:10.1109/TASC.2010.2088350
- [11] R. Di Leo *et al.*, “Niobium-titanium nitride thin films for superconducting rf accelerator cavities”, *J. Low Temp. Phys.*, vol. 78, pp. 41-50. doi:10.1007/BF00682108
- [12] N. Tsavdaris *et al.*, “A chemical vapor deposition route to epitaxial superconducting NbTiN thin films”, *Chem. Rev.*, vol. 29, pp. 5824-5830, 2017.  
doi:10.1021/acs.chemmater.7b00490
- [13] L. Yu *et al.*, “Fabrication of niobium titanium nitride thin films with high superconducting transition temperatures and short penetration lengths”, *IEEE Trans. Appl. Supercond.*, vol. 15, pp. 44-48, 2005.  
doi: 10.1109/TASC.2005.844126
- [14] A. Darlinski and J. Halbritter, “Angle-resolved XPS studies of oxides at NbN, NbC, and Nb surfaces”, *Surf. Interface Anal.*, vol. 10, pp. 223-237, 1987.  
doi:10.1002/sia.740100502
- [15] G. Jouve *et al.*, “XPS study of NbN and (NbTi)N superconducting coatings”, *Thin Solid Films*, vol. 287, pp. 146-153, 1996. doi:10.1016/S0040-6090(96)08776-7
- [16] E. Galvanetto *et al.*, “XRD and XPS study on reactive plasma sprayed titanium-titanium nitride coatings”, *Thin Solid Films*, vol. 384, pp. 223-229, 2001.  
doi:10.1016/S0040-6090(00)01871-X